JOURNAL OF MATERIALS SCIENCE 30(1995) 1111–1116

Plasticity of styrene–co-methylmethacrylate random copolymers

J. M. GLOAGUEN, B. ESCAIG, J. M. LEFEBVRE
Laboratoire de Structure et Propriétés de l'Etat Solide, URA CNRS 234, Université des Sciences et Technologies de Lille, 59655 Villeneuve d'Ascq, France

The plastic deformation of styrene–methylmethacrylate random copolymers has been studied as a function of comonomer composition and compared to the behaviour of PS and PMMA homopolymers. Activation parameters derived from a thermodynamic and kinetic analysis of plastic flow reveal the strong influence of the MMA units in controlling the elementary deformation event.

1. Introduction

The plastic deformation behaviour of random copolymers of styrene (STY) and methylmethacrylate (MMA) has been studied by compression at constant strain rate over the temperature range $170 < T < 350$ K. This work is part of a joint research programme aimed at a better understanding of the mechanical properties of these materials in relation to their chemical structure and basic physical properties.

Although they are both amorphous and display rather similar glass transition temperatures, the parent homopolymers, polystyrene (PS) and polymethylmethacrylate (PMMA), exhibit pronounced differences in their non-elastic deformation response. This is well illustrated in the observed shear-band morphologies obtained for comparable deformation conditions [1, 2], and also from a phenomenological point of view in the study of the thermally activated yielding behaviour [3, 4]. This distinction is further confirmed from the degree of anisotropy retained at the molecular level as deduced from small-angle neutron scattering experiments. Deformation bands obtained at the same strain rate and temperature in PS and PMMA have been characterized by this technique and apparent radius of gyration measurements establish the existence of a marked coil anisotropy in the case of PS, whereas rather isotropic scattering in the case of PMMA is indicative of a diffuse zone deformation regime [5]. Refering to these previous results, we have conducted a thermodynamic and kinetic analysis of the plastic flow process as a function of comonomer composition.

2. Thermodynamics and kinetics of yielding

This approach has been widely documented and is shown to provide meaningful information on the respective roles played by chain flexibility and local chain dynamics in the observed plastic deformation behaviour. Examples include amorphous and semi-crystalline thermoplastics as well as cross-linked networks [3, 4, 6–8]. We shall briefly recall the basic features of the theory.

2.1. Thermodynamics of plastic flow

In the proposed formalism, plasticity is viewed as resulting from the development of microshear bands past local obstacles characterized by an energy barrier, ΔG_0. These barriers are overcome under the combined action of stress and thermal fluctuations. The corresponding Arrhenius equation for the non-elastic strain rate is thus written

$$\dot{\varepsilon}_p = \dot{\varepsilon}_0 \exp\left(\frac{-\Delta G_a(\sigma_a - \sigma_i, T)}{kT}\right) \quad (1)$$

in which ΔG_a is the activation free energy, and the effective stress $\sigma_e = \sigma_a - \sigma_i$ is the thermal component of the flow stress, σ_a. We thus distinguish the temperature and strain-rate dependent effective stress $\sigma_e(T, \dot{\varepsilon}_p)$, from the average internal stress term, σ_i, which originates from the molecular misfits left behind the propagation front of the deformation band. In contrast to σ_e, σ_i is not thermally activated and its temperature dependence stems from that of the shear modulus, μ.

Apart from the activation free energy, we have access to its partial derivatives with respect to stress and temperature, namely the activation volume, V_a, which refers to the spatial extension of the barrier, and the activation entropy, ΔS_a.

Equation 1 can then be expressed as

$$\Delta G_a = \alpha kT \quad (2)$$

with $\alpha = \log(\dot{\varepsilon}_0/\dot{\varepsilon}_p)$, thus implying that ΔG_a is proportional to temperature in a constant strain-rate test. As recalled above, the barrier is overcome by the combined contributions of the thermal energy and mechanical work, which means that ΔG_0 may be expressed by

$$\Delta G_0 = \alpha kT + V_a \sigma_e \quad (3)$$

0022–2461

Finally, one additional parameter is of particular interest, namely the "athermal" temperature, T_a. It corresponds to the situation when the thermal fluctuations alone are strong enough to overcome the energy barrier, i.e. the effective stress is zero. Considering Equations 2 or 3 in that case, we find

$$\Delta G_0 = \alpha k T_a \quad (4)$$

and knowledge of T_a thus provides a direct measure of the barrier height [6].

The free energy of activation, may be computed as follows

$$\Delta G_a = \left(\Delta H_a + \frac{T}{\mu}\frac{d\mu}{dT}\sigma_a V_a\right)\Big/\left(1 - \frac{T}{\mu}\frac{d\mu}{dT}\right) \quad (5)$$

where ΔH_a is the activation enthalpy.

2.2. Yielding kinetics

The kinetic aspects of the rate equation are also of great matter. The non-elastic strain rate may be rewritten as

$$\dot{\varepsilon}_p = \varepsilon_0 N \nu_{def} \quad (6)$$

where N is the number of active sites, ε_0 is the volume average strain contributed by each successful event and ν_{def} is the activation rate, that is the number of shear nuclei that achieve expansion per unit time. It is the product of an attempt frequency, ν_N, by a Boltzmann term $\exp -(\Delta G_a/kT)$. If Equation 2 is valid, we thus have

$$\nu_{def} = \nu_N \exp - \alpha \quad (7)$$

The self consistency of the present analysis implies that the elastic response of the material should be measured at a frequency $\nu_{mod} = \nu_{def}$. Because ν_{def} is not known *a priori*, an iterative procedure has been designed through which the Gibbs free energy of activation is evaluated from Equation 5 with elastic modulus data, $\mu(T)$, obtained at various frequencies [9, 10].

2.3. Operational parameters

Apart from the flow stress, σ_a, and the shear modulus, μ, two additional parameters are required to compute Equation 4. These are the operational activation volume, V_0, and the operational activation enthalpy, ΔH_0. V_0 represents the stress sensitivity of the strain rate

$$V_0 = kT\left(\frac{\partial \log(\dot{\varepsilon}_p)}{\partial \sigma}\right)_{T,\,structure} \quad (8)$$

whereas ΔH_0 represents its temperature sensitivity, i.e.

$$\Delta H_0 = kT^2\left(\frac{\partial \log(\dot{\varepsilon}_p)}{\partial T}\right)_{\sigma,\,structure} \quad (9)$$

Because $\dot{\varepsilon}_0$ is generally weakly dependent on T, we have $\Delta H_0 = \Delta H_a$. Regarding V_0, the situation is not as simple and a possible stress dependence of the pre-exponential factor in Equation 1 may not be ignored. A reduced variable integration method has been proposed in the literature which enables one to compute ΔG_a from V_0 [11]. Comparison of this approach with the straightforward calculation from Equation 5 allows determination of the temperature domain for which V_0 has the meaning of a true activation volume, V_a, and also confirms the validity of the ΔG_a values.

The whole procedure is illustrated below for three STY/MMA copolymer compositions.

3. Experimental procedure

The copolymers used in this cooperative programme were obtained from Norsolor. The molecular characteristics of these materials, including comonomer composition, molecular weight and monomer sequence distributions have been reported previously. Regarding the latter, ^{13}C NMR spectroscopy results clearly confirm the random nature of the copolymers [12]. Table I gathers some of these data, i.e. molecular weights derived from GPC and glass transition temperatures taken as the 1 Hz loss modulus, T_α maximum.

The polymer powders were compression moulded under vacuum in a Darragon press at $T_g + 80$ K in the form of 3 mm thick plaques. Parallelepipedic samples with dimensions 3 mm × 3 mm × 6 mm were prepared for the constant strain-rate compression tests in an Instron machine. A few cylindrical samples with diameter 6 mm were also moulded directly in a separate equipment. After a 2 h annealing treatment at $T_g + 20$ K and slow cooling through T_g, no residual birefringence could be observed in either type of specimen, and it was thus assumed that all samples are free of internal stresses linked to the elaboration procedure.

The imposed strain rate was taken as $\dot{\varepsilon} = 1.5 \times 10^{-4}\ s^{-1}$, in order to allow comparison with the published data on PS and PMMA [3, 4]. Experimental results did not show any effect of sample geometry.

4. Results

4.1. Stress–strain behaviour

The first crucial step in the present analysis is to provide a proper definition of the flow stress, σ_y, in

TABLE I Copolymer characterization

Copolymer	Sty units (mol %)	MMA units (mol %)	M_n (g mol^{-1})	M_w (g mol^{-1})	T_g(1 Hz) (K)
S_3M_1	75	25	62 500	137 000	379.5
S_2M_2	50	50	69 000	139 000	380
S_1M_3	25	75	98 500	193 000	388

order to measure activation parameters as a function of temperature at comparable steady-state microstructures. As illustrated in Fig. 1a and b at 233 and 313 K, respectively, the apparent shape of the stress–strain curves may change quite significantly, i.e. may or may not exhibit strain-softening. For this reason an operational definition of the plastic flow stress was given some years ago (for example [3]). We chose to consider the stress level at which the experimental activation volume measured along the stress–strain curve reaches a plateau value. It corresponds either to the lower yield point when strain-softening occurs, or to the plateau value as seen for instance for S_1M_3 in Fig. 1a.

According to this definition, the flow stress data have been obtained for the three copolymers in the temperature range between 150 and 350 K. The results are presented in Fig. 2. Also shown on the same curve are the data obtained for PS and PMMA in the laboratory. The stress–temperature curves of the copolymers lie in between those of the parent polymers. The curvature of the plot in the case of S_1M_3 parallels that of PMMA whereas a linear stress–temperature variation is seen for S_3M_1 as for PS.

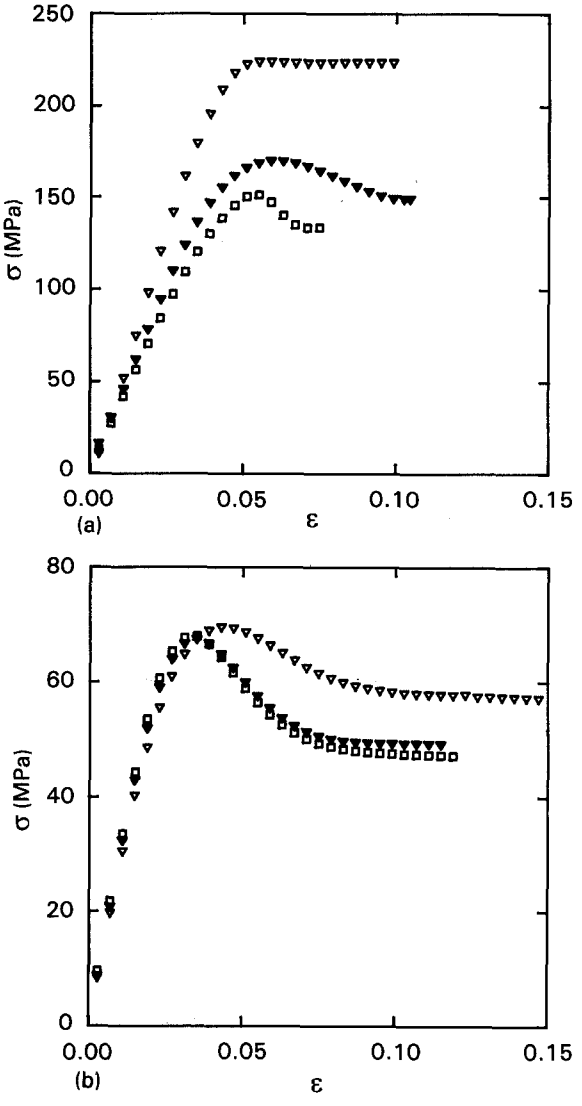

Figure 1 Typical stress–strain curves at (a) 233 K, and (b) 313 K. (▽) S_1M_3, (▼) S_2M_2, (□) S_3M_1.

4.2. Operational activation parameters

The operational activation volume, V_0, is deduced from a stress relaxation test under stationary plastic flow conditions. The plots of Fig. 3 compare the evolutions of V_0 as a function of temperature for the five materials under consideration. (V_0 is expressed with respect to the compressive stress, which means that shear activation volumes correspond to twice that quantity.) It is seen that V_0 remains fairly constant in the low-temperature domain, below 250 K for all polymer systems, and then rises rapidly with T.

The operational activation enthalpy, ΔH_0, is computed from V_0 and from the slope of the plot of the flow stress as a function of T, that is

$$\Delta H_0 = -TV_0 \, d\sigma/dT \qquad (10)$$

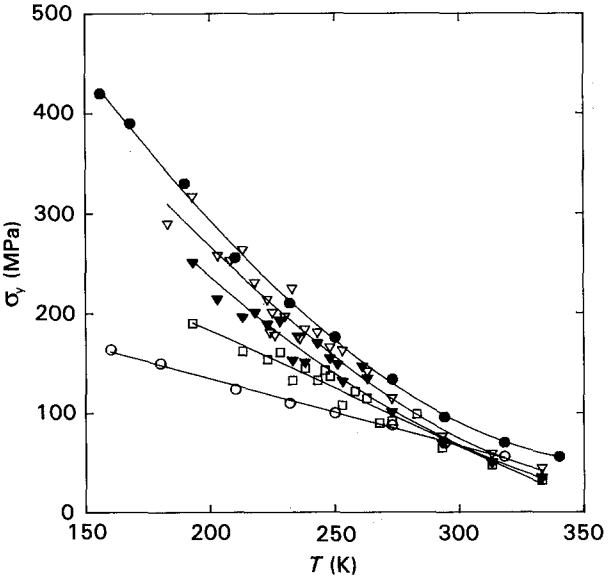

Figure 2 Yield stress as a function of temperature for the homopolymers and the three copolymers. (○) PS, (●) PMMA, (▽) S_1M_3, (▼) S_2M_2, (□) S_3M_1.

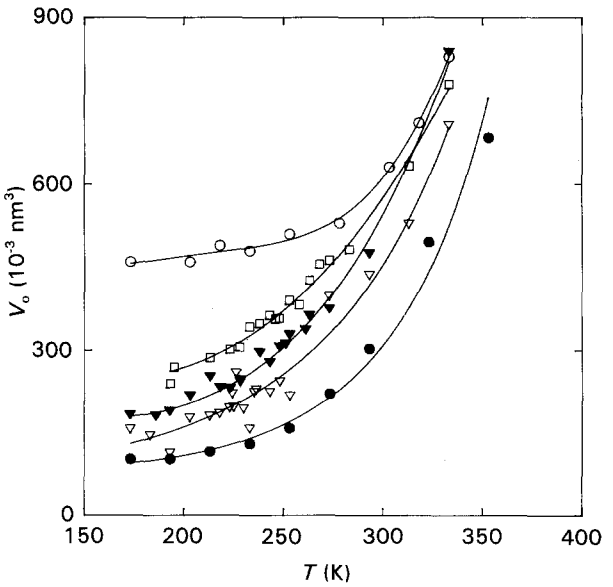

Figure 3 Temperature dependence of the operational activation volume for the homopolymers and the three copolymers. For key, see Fig. 2.

which stems directly from the definitions of V_0 and ΔH_0 given earlier.

4.3. Free energy of activation

The determination of the Gibbs free energy of activation is then achieved according to Equation 5. As mentioned in the presentation of the kinetic aspects of the rate equation the self-consistent frequency, ν_{mod}, at which the elastic response of the materials has to be measured is not known; however, in the present case, our previous results for PS and PMMA give $\nu_{mod} = \nu_{def}$ of the order of 10^3 Hz. For this reason the temperature variation of the elastic modulus of the three copolymers has been measured in a tension–compression mode at a frequency of 500 Hz on a Metravib viscoelasticimeter. The plots of the temperature evolutions of the activation enthalpy and free energy are presented in Figs 4–6 for the three copolymers. ΔG_a values have also been computed from the direct integration of the operational activation volume. The results, not shown on these graphs for the sake of clarity, indicate agreement between the two routes for temperatures up to 250–270 K. Thus, in the low-temperature range of experimental data, $V_0 = V_a$ has the physical meaning of the spatial extension of the thermally activated deformation event. Regarding this temperature limit, it is not possible to differentiate the copolymers within experimental error.

Returning to the ΔG_a versus T plots, we find a linear variation with a straight line going through the origin, thus fulfilling Equation 2 up to 250–270 K. Moreover the slope $\alpha = 21$–22 yields an elementary deformation frequency in the range $200 < \nu_{def} < 800$ Hz perfectly consistent with the frequency of modulus determination.

As a final comment on Figs 4–6, it is clearly seen that the difference between enthalpy and free energy, i.e. the entropy term increases in magnitude as the MMA content is varied from 25 mol % to 75 mol %.

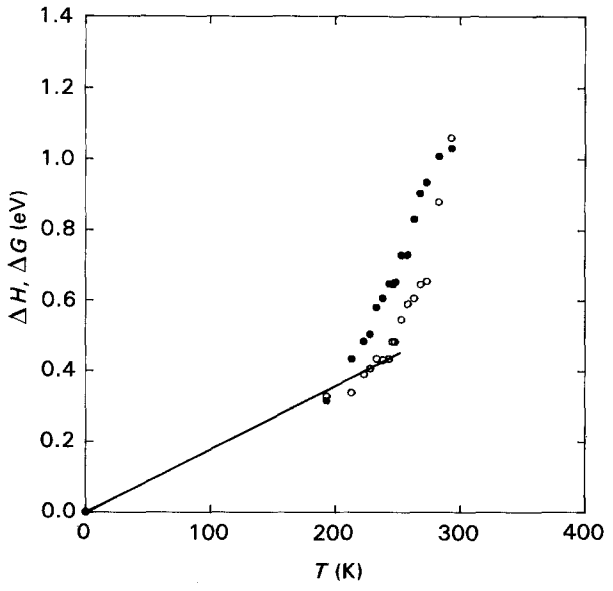

Figure 4 Temperature dependence of the (●) activation enthalpy and (○) free energy in the case of S_3M_1.

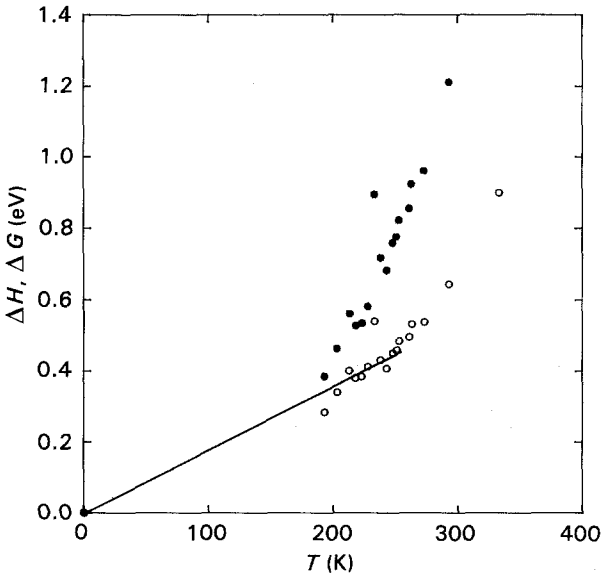

Figure 5 Temperature dependence of the (●) activation enthalpy and (○) free energy in the case of S_2M_2.

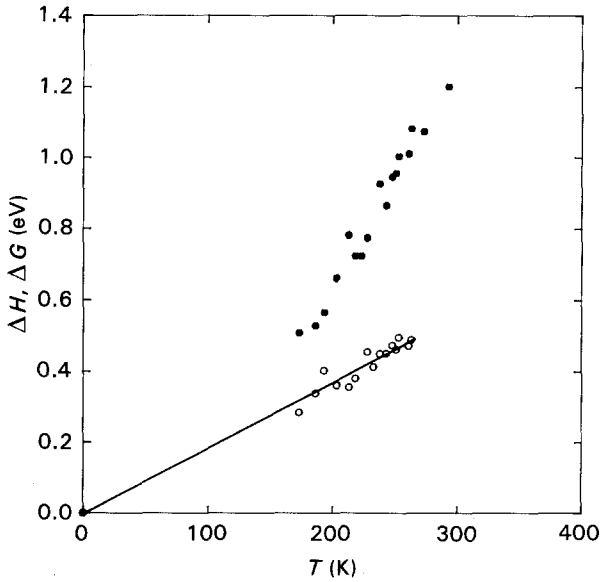

Figure 6 Temperature dependence of the (●) activation enthalpy and (○) free energy in the case of S_1M_3.

4.4. Energy barrier, ΔG_0

The magnitude of the local energy barrier, ΔG_0, may be obtained from Equation 4 which requires knowledge of the athermal temperature, T_a. It has been shown that V_0 should tend to infinity as T approaches T_a. Instead of trying to guess the temperature at which divergence occurs on the $V_0(T)$ plot, it is more fruitful to study the evolution with T of the parameter $\lambda = kT/V_0$. The latter quantity tends towards zero at T_a, and based on simple arguments it may be justified that a polynomial fit of degree two accounts for the $\lambda(T)$ data [6]. These plots are presented in Figs 7–9 for the copolymers and Table II gathers T_a and ΔG_0 values, including those for PS and PMMA. Fig. 10 illustrates their evolutions as a function of the molar % of MMA units.

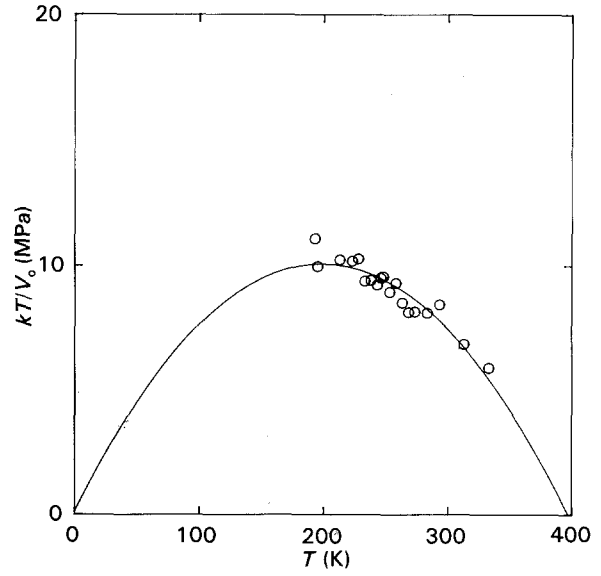

Figure 7 Evolution of kT/V_0 versus T in the case of S_3M_1.

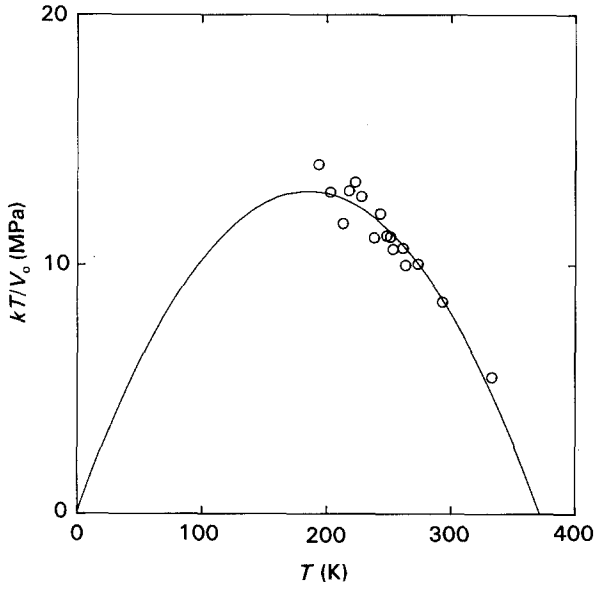

Figure 8 Evolution of kT/V_0 versus T in the case of S_2M_2.

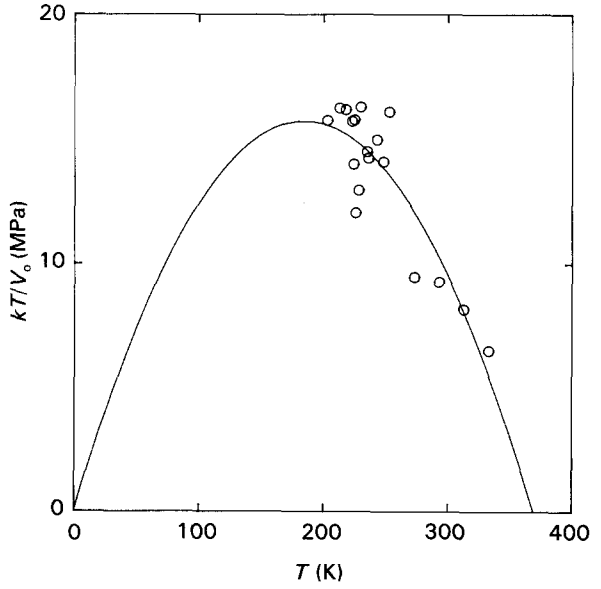

Figure 9 Evolution of kT/V_0 versus T in the case of S_1M_3.

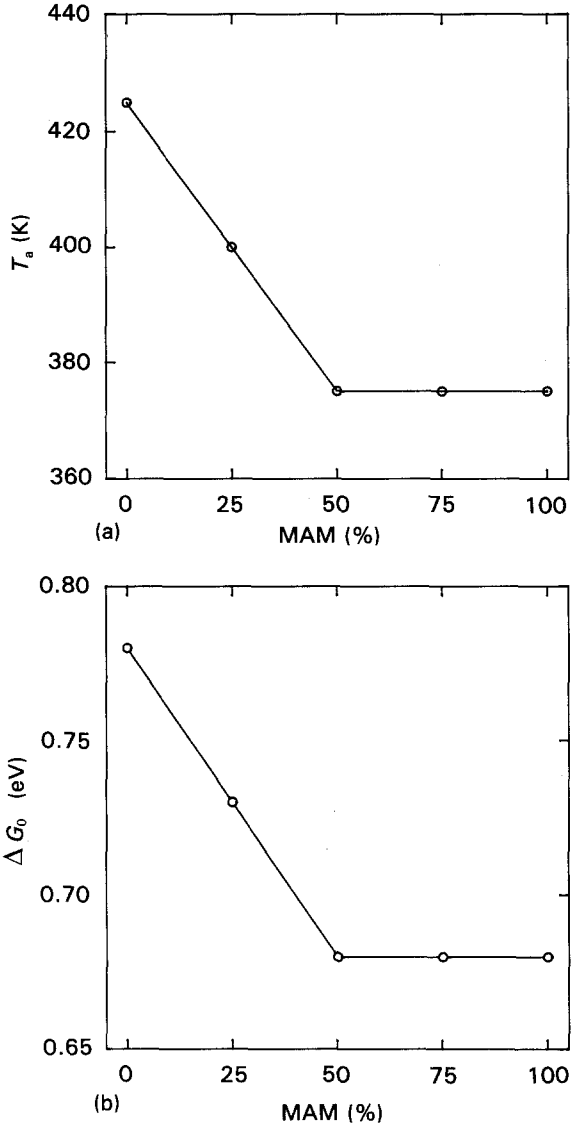

Figure 10 Variation of (a) T_a and (b) ΔG_0 as a function of the fraction of MAM units (expressed in mol %).

TABLE II Activation parameters

Copolymer	T_a (K)	ΔG_0 (eV)
PS	425	0.78
S_3M_1	400	0.73
S_2M_2	375	0.68
S_1M_3	375	0.68
PMMA	375	0.68

5. Discussion

It is first important to recall that the homopolymers exhibit markedly distinct behaviours regarding the whole set of activation parameters under consideration. The slopes of the $\sigma_y(T)$ plots and consistently the low-temperature true-activation volumes, V_a, differ by a factor of the order of 4 (0.9 nm^3 for PS and 0.22 nm^3 for PMMA, where V_a is expressed in shear). Also the extrapolated flow stress at 0 K amounts to roughly 280 MPa in PS, compared with 850 MPa in PMMA [3, 4].

In the low-temperature regime, the intermediate behaviour shown in Figs 2 and 3 by the $\sigma_y(T)$ and

$V_a(T)$ plots of the copolymers obviously does not obey a simple rule of mixtures of the corresponding homopolymer properties. On the contrary, it reveals a dominant role of the MMA sequences in the rate-controlling deformation process. For example, referring to the values given above, the incorporation of only 25% MMA units results in a drop of the activation volume to about 0.460 nm^3, and V_a becomes still closer to the value for PMMA in the case of S_2M_2 (0.340 nm^3) and S_1M_3 (0.270 nm^3).

A dislocation approach has been taken to model these activation parameters in terms of local chain structure and molecular dynamics [13]. It is considered that the major steric hindrances to relative chain motions in the propagation of shear bands come from entanglements. Reducing the bad molecular misfits caused by these points implies to have them moved off the slip interface. Taking $\langle \boldsymbol{b} \rangle$ as the average Burgers vector (shift) of the band, removal of the entanglement from the slip interface may be viewed as the nucleation of an additional prismatic dislocation loop of Burgers vector $\beta = \boldsymbol{b}(M) - \langle \boldsymbol{b} \rangle$, where $\boldsymbol{b}(M)$ is the local Burgers vector at point M. In the frame of this picture of Somigliana dislocations in polymeric glasses, the activation volume is related to the area swept by the β-loop up to its critical configuration. The radius of the zone of hindrance obviously depends on local chain stiffness and it has been proposed to take it as the length, s, of the statistical chain element [13]. The activation volume is thus expressed as

$$V_a = f\beta s^2 \qquad (11)$$

in which f is a stress-dependent factor of the order of unity and less than π. Experimental comparison for vinyl thermoplastics as well as epoxy networks, gives a constant ratio $V_a/s^2 \approx 1.9$ [14].

Returning to the polymers of concern here, with $s_{PS} \approx 2s_{PMMA}$, agreement is found with the ratio of four in the activation volumes. To date, no data are available concerning the persistence lengths of the statistical copolymers, but rotational isomeric states calculations are in progress in the cooperative programme [15] and should allow further testing of the dislocation model in the near future.

The dominant influence of MMA units is also revealed in the ΔG_0 values of Fig. 10, as well as in the T_as. The latter quantities may seem somewhat surprising for PS and S_3M_1, because they are higher than T_g; however, it simply indicates at which temperature the local energy barrier would have been overcome by coherent thermal fluctuations alone, had not the molecular motions of the glass transition been activated.

Finally these plasticity findings may also be considered on a structural basis in the light of the X-ray work by Mitchell and co-workers [16] who studied the local structure of such random STY/MMA copolymers. It seems particularly pertinent to the above comments that the preferential stacking of phenyl groups in polystyrene giving the so-called "superchain" structure [16] is preserved in the 75/25 (S_3M_1) copolymer, whereas the S_2M_2 type copolymer has lost these correlated structures.

Acknowledgement

The cooperative research programme is supported by the Centre National de la Recherche Scientifique: GDR 933-"Relations structure-propriétés mécaniques des polymères".

References

1. J. C. M. LI, in "Plastic Deformation of Amorphous and Semicrystalline Materials", edited by B. Escaig and C. G'Sell (Les éditions de physique, Les Ulis, 1982) p. 29.
2. P. B. BOWDEN, in "The physics of glassy polymers", edited by R. N. Haward (Applied Science, London, 1973).
3. J. P. CAVROT, J. HAUSSY, B. ESCAIG and J. M. LEFEBVRE, *Mater. Sci. Eng.* **36** (1978) 95.
4. J. HAUSSY, J. P. CAVROT, J. M. LEFEBVRE and B. ESCAIG, *J. Polym. Sci, Polym. Phys.* **18** (1980) 311.
5. J. M. LEFEBVRE, B. ESCAIG, G. COULON and C. PICOT, *Polymer* **26** (1985) 1807.
6. K. PORZUCEK, J. M. LEFEBVRE, G. COULON and B. ESCAIG, *J. Mater. Sci.* **24** (1989) 3154.
7. D. MELOT, Thèse de Doctorat en Sciences des Matériaux, Université de Lille (1989).
8. F. FERNAGUT, Thèse de Doctorat en Sciences des Matériaux, Université de Lille (1990).
9. B. ESCAIG, in "Plastic Deformation of Amorphous and Semicrystalline Materials", edited by B. Escaig and C. G'Sell (Les éditions de physique, Les Ulis, 1982) p. 187.
10. J. M. LEFEBVRE and B. ESCAIG, *J. Mater. Sci.* **20** (1985) 438.
11. M. CAGNON, *Philos. Mag.* **30** (1971) 1465.
12. J. L. HALARY, A. K. OULTACHE, J. F. LOUYOT, B. JASSE, T. SARRAF and R. MULLER, *J. Polym. Sci. Polym. Phys.* **29** (1991) 933.
13. B. ESCAIG, in "Dislocations in solids", Yamada Science Foundation, edited by H. Suzuki (University of Tokyo Press, Tokyo, 1985) p. 559.
14. J. M. LEFEBVRE and B. ESCAIG, *Polymer* **34** (1993) 518.
15. F. LAUPRÊTRE and L. MONNERIE, ESPCI Paris personal communication (1992).
16. G. R. MITCHELL, A. D. PROCTOR and A. GILBERT, *J. Polym. Sci. Polym. Lett.* **28** (1990) 423.

Received 25 June 1992
and accepted 3 February 1993